Polymer 51 (2010) 3445–3452

Contents lists available at ScienceDirect

Polymer

journal homepage: www.elsevier.com/locate/polymer

Adsorption of anionic amphiphilic polyelectrolytes onto amino-terminated solid surfaces

M.D. Urzúa [a,*], X.G. Briones [a], L.P. Carrasco [a], M.V. Encinas [b], D.F.S. Petri [c]

[a] Departamento de Química, Facultad de Ciencias, Universidad de Chile, Las Palmeras 3425, Casilla 653, Santiago, Chile
[b] Facultad de Química y Biología, Universidad de Santiago de Chile, Santiago, Chile
[c] Instituto de Química, Universidade de São Paulo, P.O. Box 26077-05599-970, São Paulo-SP, Brazil

ARTICLE INFO

Article history:
Received 26 March 2010
Received in revised form
20 May 2010
Accepted 25 May 2010
Available online 2 June 2010

Keywords:
Amphiphilic polyelectrolytes
Amino-terminated surface
Surface adsorption

ABSTRACT

The adsorption behavior of several amphiphilic polyelectrolytes of poly(maleic anhydride-alt-styrene) functionalized with naphthyl and phenyl groups, onto amino-terminated silicon wafer has been studied by means of null- ellipsometry, atomic force microscopy (AFM) and contact angle measurements. The maximum of adsorption, $\Gamma_{plateau}$, varies with the ionic strength, the polyelectrolyte structure and the chain length. Values of $\Gamma_{plateau}$ obtained at low and high ionic strengths indicate that the adsorption follows the "*screening-reduced adsorption*" regime. Large aggregates were detected in solution by means of dynamic light scattering and fluorescence measurements. However, AFM indicated the formation of smooth layers and the absence of aggregates. A model based on a two-step adsorption behavior was proposed. In the first one, isolated chains in equilibrium with the aggregates in solution adsorbed onto amino-terminated surface. The adsorption is driven by electrostatic interaction between protonated surface and carboxylate groups. This first layer exposes naphtyl or phenyl groups to the solution. The second layer adsorption is now driven by hydrophobic interaction between surface and chains and exposes carboxylate groups to the medium, which repel the forthcoming chain by electrostatic repulsion. Upon drying some hydrophobic naphtyl or phenyl groups might be oriented to the air, as revealed by contact angle measurements. Such amphiphilic polyelectrolyte layers worked well for the building-up of multilayers with chitosan.

1. Introduction

Amphiphilic polyelectrolytes have been viewed as polysoaps because their monomeric structure is similar to that of a simple, low-molecular weight, surfactant molecule. Consequently, it is possible to observe analogous behavior to that in micellar system. However, polysoaps do not show a critical micelle concentration because each macromolecule represents a "preformed micelle" containing quasi-micellar clusters due to hydrophobic interactions between aliphatic side chains [1,3]. This type of polyelectrolytes has been of great interest for basic as well as applied science [4]. These systems present self-assembling phenomena in aqueous environment, which is governed by electrostatic forces, hydrogen bonds, van der Waals, and hydrophobic interactions [4,5]. Consequently, this particular property that these systems present allows describing and studying different biological phenomena. Amphiphilic copolymers of maleic acid and monomers such as alkyl vinyl ethers, styrene and derivatives, and methacrylic acid are widely used as surfactants and materials for biomedical applications [2,6–11]. The stabilization of these materials in bulk solution is related to their ability to hypercoil by hydrophobic interaction.

The use of polyelectrolytes in the modification of solid surfaces [12–15], forming monolayers or multilayers with multiple interfacial structures, modulates the function and structure of such layers, opens a vast field of technological applications, as for instance in paper making strength additives, flocculating agents in waste water treatment, surface conditioning, food processing, biotechnology, and medicine [16–21].

Few studies have been performed about the adsorption behavior of amphiphilic polyelectrolytes onto amino-terminated surfaces [22]. The structural and functional properties of these polyelectrolyte layers adsorbed on solid substrates depend on the conformation of polyelectrolyte chains bonded to the solid substrate, and their adsorption behavior depends on parameters such as polymer charge density, surface charge density, pH and ionic strength on the medium from which the polyelectrolyte is adsorbed [14,15,23–28]. For instance, the adsorption of carboxymethylcellulose onto amino-terminated Si wafers is favored by pH

* Corresponding author. Tel.: +56 2 9787444; fax: +56 2 2738888.
E-mail address: maurzua@uchile.cl (M.D. Urzúa).

0032-3861/$ – see front matter © 2010 Elsevier Ltd. All rights reserved.
doi:10.1016/j.polymer.2010.05.054

lower than 4 and low ionic strength [29]. On the other hand, the adsorption of poly(4-vinylpyridine) N-ethyl or N- pentyl quaternized, QPVP-C2 or QPVP-C5, respectively, onto Si/SiO_2 wafers was favored upon increasing the ionic strength [30]. Specially QPVP-C5 layers with the longer alkyl lateral group worked well as support for lysozyme adsorption. Antimicrobial effects observed for pure lysozyme layers were comparable to those observed for QPVP-C5 or QPVP-C2 layers [30].

Van de Steeg and co-workers [31] developed a theory for the polyelectrolyte adsorption based on numerical calculations, which consider salt concentration, segment charge and surface charge. This theory describes two regimes. The first is the so-called *screening-reduced adsorption* regime, where the adsorbed amount decreases with increasing salt concentration. This regime has been found for polyelectrolytes with low as well as with high segment charge and sufficiently high surface charge density. This effect is expected if the attraction between polyelectrolyte and surface is mainly electrostatic, since salt screens not only the segment–segment repulsion but also the segment-surface attraction. The second is the *screening-enhanced adsorption* regime, where the adsorbed amount increases with increasing salt concentration. This case has been often found for highly charged polyelectrolyte. The idea is that at high salt concentration the strong segment repulsion is screened and the polyelectrolyte chains behave more like uncharged polymers. Hence, they can adopt conformations like loops and tails, increasing the adsorbed amount. This situation is favored only if there is an attractive interaction between segments and surface, which is not electrostatic in nature.

With the aim of obtaining new materials for polymeric films of negatively charged polyelectrolytes onto positive charged surface, in the present work we study the adsorption behavior of anionic amphiphilic polyelectrolytes derivative from poly(maleic anhydride-alt-styrene) modified with phenyl or naphthyl groups as side chain (Scheme 1) onto amino-terminated silicon wafer surface. The effect of ionic strength and the chain length on the adsorption behavior was investigated by means of ellipsometry. The adsorbed layers were characterized by means of contact angle measurements and atomic force microscopy (AFM).

2. Experimental part

2.1. Synthesis and materials

High molecular weight (M_v 125,000 g/mol) poly(maleic anhydride-alt-styrene), P(MA-alt-S), was synthesized by free radical polymerization in anhydrous benzene at 55 °C under nitrogen atmosphere, mixing equimolar amounts of maleic anhydride and styrene, and using α,α-azobis(isobutyronitrile) as initiator. Average molecular weight was determined by solution viscosity measurements in THF at 30 °C, considering the Mark-Houwink-Sakurada constants as $a = 0.81$ and $K = 5.07 \times 10^{-5}$ [32]. Low molecular weight P(AM-alt-S) (M_v 1600 g/mol) was purchased from Aldrich, Milwaukee, USA. These copolymers were functionalized with phenyl (Ph) or naphthyl (N) groups, by refluxing with the respective aromatic alcohol in acetonitrile/THF (80/20). Reactions were considered completed when in the IR spectra of the copolymer the 1654 (phenyl) and 1636 cm^{-1} (naphthyl) bands due to the ester carbonyl group appeared in place of the 1856 and 1779 cm^{-1} bands due to the maleic anhydride carbonyl group (see supplementary materials). Further evidence of the completed functionalization (~99%) was obtained from ^{13}C NMR spectroscopy (400 MHz, DMSO). These spectra showed that bands at 172.0 and 173.2 ppm corresponding to carbon atom of the maleic anhydride carbonyl group disappear and the characteristic band of the carboxylic acid group (178.4–177.2 ppm) and that of the carbon atom of the carbonyl ester at 67.0 ppm appear.

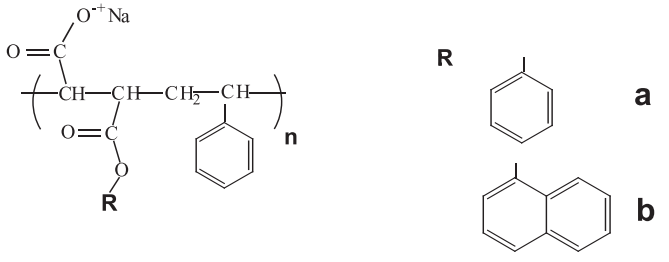

Scheme 1. Chemical structures of (a) phenyl- and (b) naphthyl- functionalized polyelectrolytes.

The sodium salts were obtained by treating the functionalized copolymers with 10% w/v $NaHCO_3$ during one week. The resulting solutions were dialyzed and lyophilized. Polyelectrolyte samples used here were coded as PPh16, PPh1250, PN16 and PN1250, Table 1.

Samples were prepared by dissolving the copolymers in deionized water at pH 4 containing 0.001 M and 0.1 M NaCl. The pH was adjusted by adding HCl. The copolymer concentration was varied from 0.01 to 1.0 g/L.

Chitosan (CH) purchased from Fluka was purified by dissolving in 0.1 M acetic acid and precipitating in 0.1 M NaOH three times. Afterwards, the CH flocs were freeze dried. CH used in this work was a copolymer composed of 20 wt.% of chitin and 80 wt.% of chitosan, the corresponding structures are shown in Scheme 2. An average molecular weight (M_v) of 218,500 g/mol was determined by viscosity in 0.1 mol/L acetic acid and 0.2 M NaCl, taking the Mark-Houwink-Sakurada constants as $a = 0.93$ and $K = 1.81 \times 10^{-3}$ [33].

Silicon (100) wafers purchased from Silicon Quest (Santa Clara, CA, USA), with a native oxide layer approximately 2 nm thick, were rinsed by standard methods [22]. Then, the surfaces were functionalized with 3-aminopropyltrimethoxysilane, APS (Fluka, Switzerland), following the method described elsewhere [22]. This method yields flat and homogeneous amino-terminated monolayers covalent bound to silicon wafers.

2.2. Methods

2.2.1. Ellipsometry

Ellipsometric measurements were performed in a vertical computer-controlled DRE-EL02 ellipsometer (Ratzeburg, Germany). The incidence angle (Φ) was set to 70°, and the laser wavelength was 632.8 nm. This equipment works as a null-ellipsometer [34]. The adsorption from solution was monitored *in situ* with the help of a cell model of poly(methyl methacrylate) [29]. The measurements were done at 23 °C ± 1 °C. The adsorbed amount (Γ) was determined from Eq. (1) [35],

$$\Gamma = \frac{d_{poly}\left(n_{poly} - n_0\right)}{dn/dc} = d_{poly}c_{poly} \quad (1)$$

where n_{poly} and d_{poly} are the refraction index and thickness of the adsorbed polyelectrolyte, n_0 is the refraction index of the solution measured with an Abbe refractometer, dn/dc is the increment of

Table 1
Sample characteristics.

Sample code	M_v (g/mol)	Side group
PPh16	1600	Phenyl
PPh1250	125,000	Phenyl
PN16	1600	Naphthyl
PN1250	125,000	Naphthyl

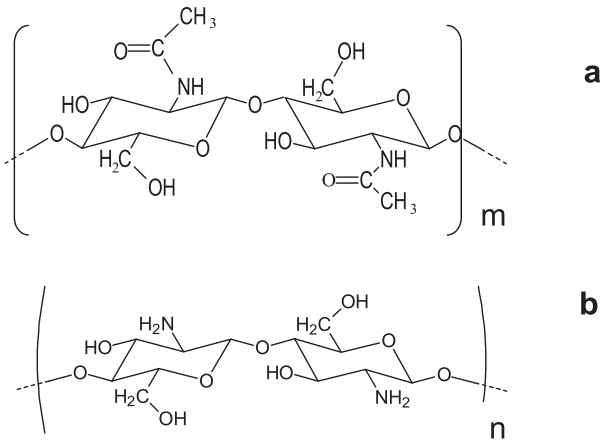

Scheme 2. Chemical structures of (a) chitin and (b) chitosan.

refractive index determined with a differential refractometer and c_{poly}, is the average polyelectrolyte concentration within the layer [35]. For our system, n_0 was measured for each concentration and dn/dc amounted to 0.16 ml/g at the temperature of 23 °C.

From the ellipsometric angles Δ and Ψ and a multilayer model composed by silicon, silicon dioxide, amino-terminated monolayer, polyelectrolyte layer and solution it is possible to determine only the thickness of the adsorbed polyelectrolyte, d_{poly}. The small differences in the refraction index of the substrate, polyelectrolyte and solution make an independent determination of n_{poly} and d_{poly} impossible. Therefore, n_{poly} was kept constant as 1.50 and d_{poly} was calculated. The hydrodynamic thickness could be calculated if the optical contrast in the system were higher. However, it is important to remember here that, if the refraction index assumed for the adsorbing polymer layer lies in a reasonable range (between 1.40 and 1.60), the product $n_{poly}d_{poly}$ should be a constant value [34,36]. This product is the necessary parameter to calculate the adsorbed amount Γ from Eq. (1). When the adsorption begins, a significant decrease in Δ and a small increase in Ψ were observed. After 3 h of adsorption, it were not observed changes in Δ or Ψ, indicating that the adsorption equilibrium was achieved.

2.2.2. Atomic force microscopy

AFM topographic images were obtained using a PicoSPM-LE Molecular Imaging system with cantilevers operating in the intermittent-contact mode (AAC mode), slightly below their resonance frequency of approximately 290 kHz in the air. All topographic images represent unfiltered original data and refer to scan areas of 1 μm × 1 μm with a resolution of (512 × 512) pixels. At least two samples of the same material were analyzed at different areas of the surface. Image processing and the determination of the root mean square (rms) roughness were performed by using the PicoScan 5.3.2. software.

2.2.3. Contact angle

Contact angle measurements were performed in a home-built apparatus equipped with a digital camera, connected to a computer. Sessile water drops of 8 μL and 4 μL were used for advancing (θ_A) and receding (θ_R) angle, respectively. The hysteresis in the contact angle ($\Delta\theta = \theta_A - \theta_R$) stems from surface roughness or surface chemical heterogeneities.

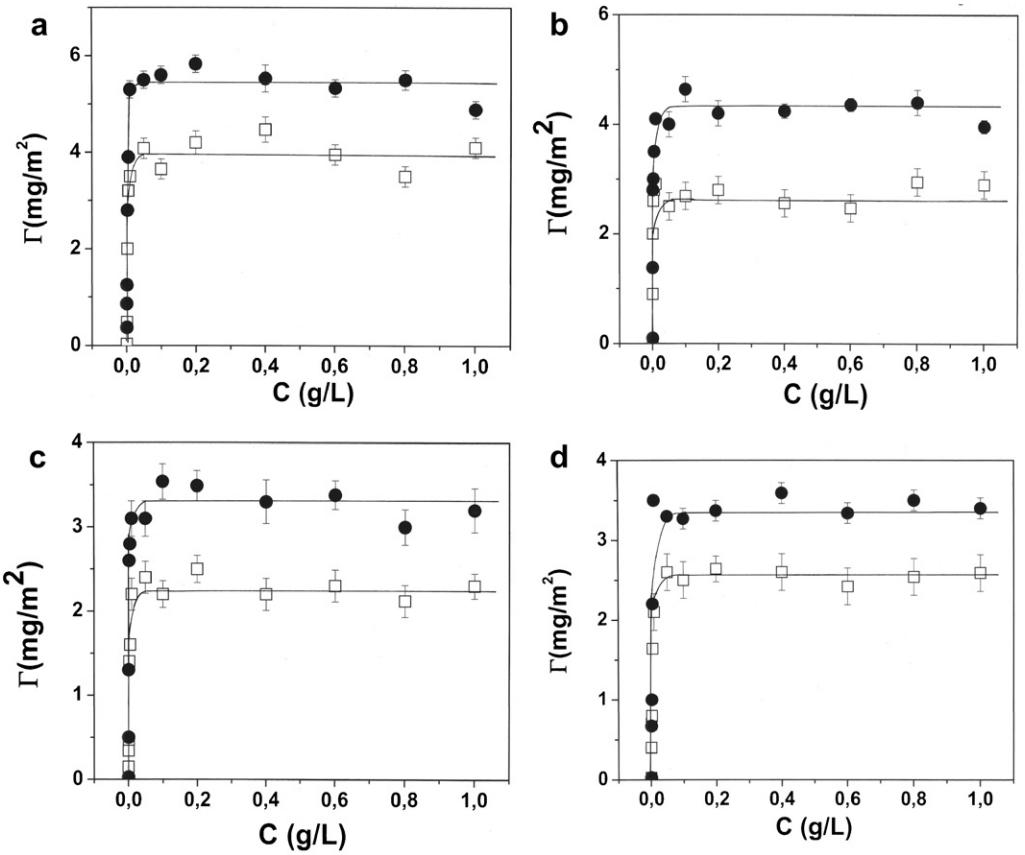

Fig. 1. Adsorption isotherms obtained for (a) PPh16, (b) PPh1250, (c) PN16 y (d) PN1250 onto amino-termined surfaces at pH 4, under ionic strength of 0.1 M (□) and 0.001 M NaCl (●). The dash lines represent the adsorption plateau.

2.2.4. Dynamic light scattering (DLS)

DLS measurements were performed with a modified NICOMP model 370 Submicron particle sizer instrument. Automatic sample dilution was performed, using an Ar Ion Cyonic-Uniphase laser, model 2213-75GLYW, as light source. A variety of polydisperse latexes with known particle size distribution were previously analyzed in a Nicomp 370 in order to test the accuracy of the technique. DLS measurements were performed at 23 °C, with scattering angle of 90°, for solutions of PPh16, PPh1250, PN16 and PN1250 (0.4 g/L) dissolved in 0.1 M and 0.001 M NaCl at pH 4.

2.2.5. Fluorescence measurements

Corrected fluorescence spectra were taken with a Spex Fluorolog spectrofluorometer. All spectra were recorded at room temperature in air equilibrated solutions. Bandwidths of 1.25 nm were used for excitation and emission slits. Pyrene was used as fluorescent probe to detect the microaggregates. Pyrene was dissolved in methanol and added to empty vials. After the evaporation of the methanol, the polymer solutions were added to the vials, and were allowed to equilibrate overnight with stirring. The final pyrene concentration was 1 μM.

2.2.6. Building-up of multilayers

For the build-up of multilayers, amino-terminated surfaces (quartz slides or Si wafers) were dipped into solution of PPh16 1.0 g/L, at pH 4 and containing 0.001 M NaCl during 20 min. After that they were dipped in CH solution (1.0 g/L) in 0.001 M HCl, pH 5 during subsequent 20 min. The substrates were dipped alternately in PPh16 and CH solutions 10 times. After each immersion the samples were rinsed with pure water, dried and characterized by means of ellipsometry (multilayers on Si wafers) and UV-spectrophotometry (multilayers on quatz slides). The absorbance was measured with a Beckmann Coulter DU 640 equipment at 278 nm, where electronic transition of C=O group can be detected.

3. Results and discussion

3.1. Influence of ionic strength on the adsorption behavior

Adsorption isotherms for PPh16, PPh1250, PN16 and PN1250 onto amino-terminated surfaces at pH 4, under 0.1 M NaCl and 0.001 M are shown in Fig. 1. All experiments show high-affinity-type adsorption isotherms. Regardless the ionic strength and polymer characteristics, the adsorbed amount Γ increases with polymer concentration and reaches a plateau at the concentration of 0.05 g/L. However, the adsorbed amount at the plateau, $\Gamma_{plateau}$, varies with the medium ionic strength and the copolymer structure (Fig. 2). For all the studied copolymers the highest $\Gamma_{plateau}$ values were found at low ionic strength, indicating that the adsorption follows the "screening-reduced adsorption" regime [31]. This is a clear evidence that the interaction between the polyelectrolyte and the surface is mainly electrostatic. At pH 4, the amino-terminated surface is partially protonated (pK 3.7) [29,37] and polyelectrolyte carboxylate groups are partially deprotonated [6], leading to electrostatic attraction between substrate and polyelectrolyte.

Table 2
Apparent hydrodynamic radius R_H and apparent diffusion coefficient D obtained for PPh16, PPh125, PN16 and PN125 at the concentration of 1.0 g/L (within the adsorption plateau) at 0.1 mol/L or 0.001 mol/L NaCl.

C_{NaCl} [mol/L]	Polyelectrolyte	R_H [nm]	D (cm^2/s)
0.001	PPh16	97 ± 9	2.4×10^{-8}
	PPh1250	250 ± 25	6.0×10^{-9}
	PN16	102 ± 10	2.1×10^{-8}
	PN1250	304 ± 30	3.0×10^{-9}
0.1	PPh16	85 ± 8	5.1×10^{-8}
	PPh1250	187 ± 18	9.9×10^{-9}
	PN16	90 ± 9	3.2×10^{-8}
	PN125	175 ± 17	5.1×10^{-9}

The $\Gamma_{plateau}$ values presented in Fig. 2 are too large to be attributed to the formation of a polyelectrolyte monolayer. Two mechanisms could explain the large $\Gamma_{plateau}$ values: (i) polyelectrolyte aggregates in the solution are adsorbed onto substrate, or (ii) the first adsorbed polyelectrolyte layer attracts the adsorption of other polyelectrolyte chains, following a cooperative process [38]. This multilayer adsorption is commonly observed with proteins [39,40].

The presence of aggregates in the solution was deduced from DLS measurements. These experiments were performed for PPh16, PPh1250, PN16 and PN1250 at the concentration of 1.0 g/L (within the adsorption plateau) in 0.1 M and 0.001 M NaCl. Table 2 shows the apparent hydrodynamic radius values R_H and the apparent diffusion coefficients obtained for each polyelectrolyte. R_H values lie between 80 nm and 300 nm, indicating the presence of intermolecular aggregates in solution, probably resulting from hydrophobic interactions between aromatic side groups. Moreover, the charge and hydratation of polyelectrolytes could contribute to the large aggregates formation. At high ionic strength the R_H values are smaller than those found at 0.001 M. These findings indicate that salt screens the polyelectrolyte charges, diminishing the repulsion between charged segments and then, reducing the aggregate size.

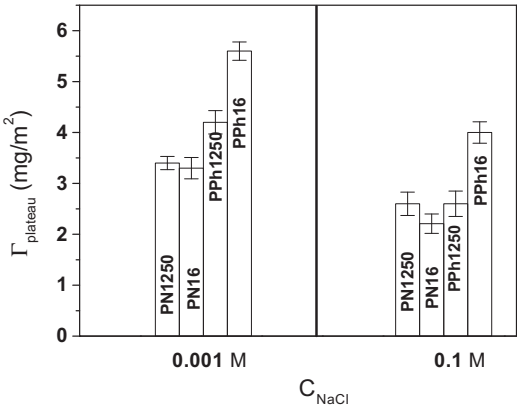

Fig. 2. Dependence of the adsorbed amount at the plateau, $\Gamma_{plateau}$, (values extracted from Fig. 1) at the ionic strength at pH 4.

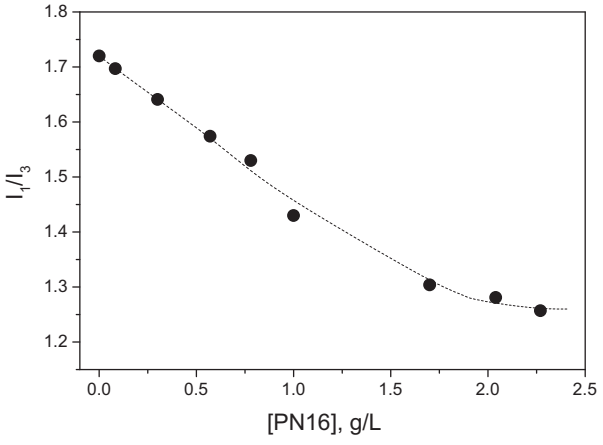

Fig. 3. Ratio of fluorescence intensity of vibronic band, I_1/I_3, of pyrene as a function of PN16 concentration.

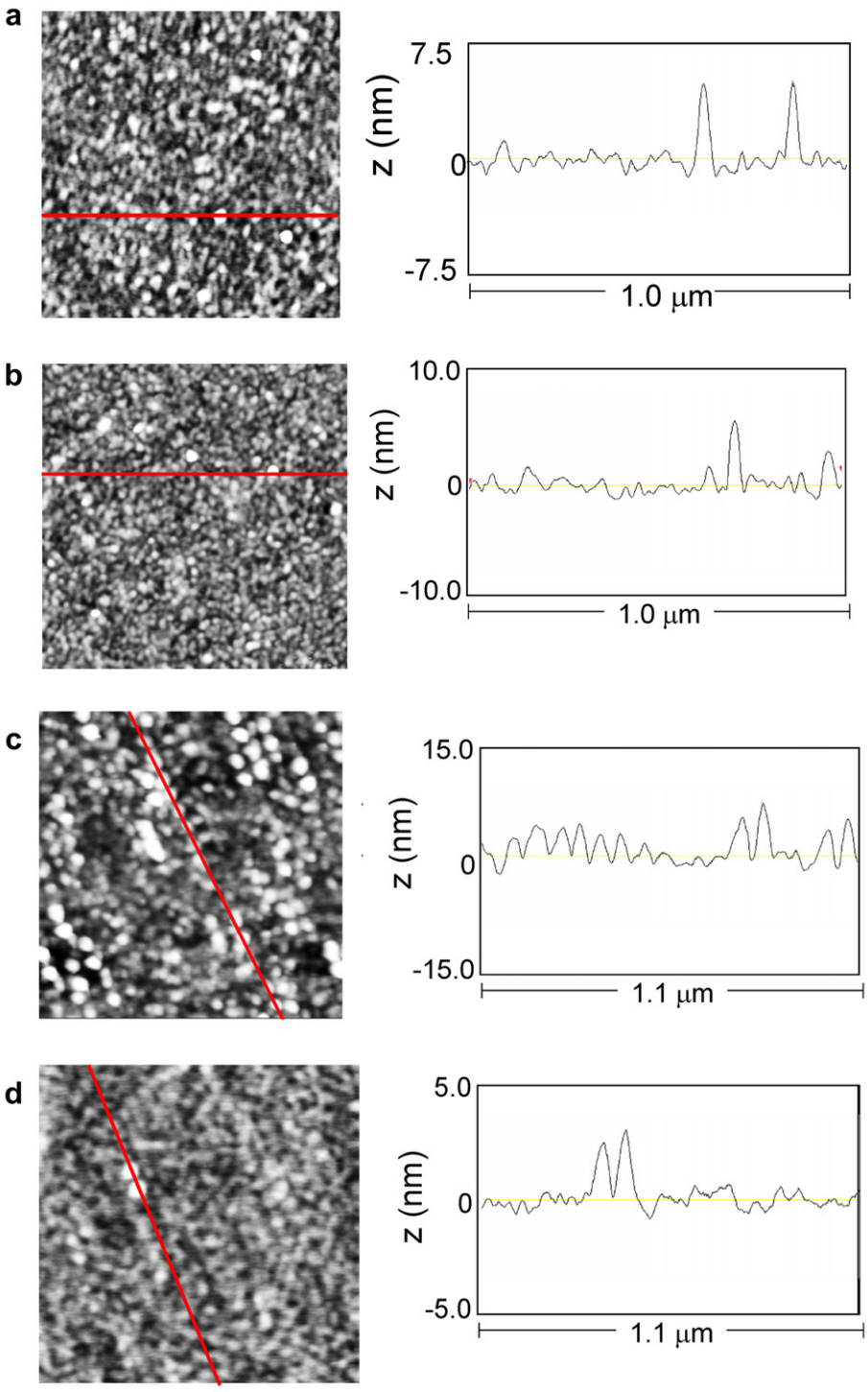

Fig. 4. AFM topographic images for (a) PN16, 0.001 M NaCl, $z = 5$ nm; (b) PN16, 0.1 M NaCl, $z = 8$ nm; (c) PPh16, 0.001 M NaCl, $z = 20$ nm; (d) PPh16, 0.1 M NaCl, $z = 6$ nm. All images correspond to scan areas of 1 μm × 1 μm.

Similarly, Samoshima et al. [26] found R_H value of 130 nm for amphiphilic copolymers of triethyl(vinylbenzyl)-ammonium chloride and dimethyldodecyl(vinylbenzyl) ammonium chloride with 80 mol % of monomer modified with dodecyl chains. They suggested that the intermolecular aggregates are formed in solution by attractive interaction between grafted dodecyl chains.

Further evidence of the presence of microaggregates in solution was assessed using pyrene as fluorescent probe. The fluorescence spectrum of pyrene probe offers a convenient mean of sensing molecule local environment. The intensity of the ratio of the first vibronic band to the third band (I_1/I_3) decreases when the medium polarity decreases. The ratio I_1/I_3 of the pyrene intensity at 374 and

385 nm was used to detect the microaggregates in the solution since the pyrene as the tendency to occupy hydrophobic sites. If hydrophobic aggregates are formed, it is expected a decrease of the ratio I_1/I_3. When low pyrene concentration (<3 μM) was solubilized in copolymer aqueous solutions at concentration higher than that employed to reach a plateau in the absorption of copolymers on the amine-terminated surface, the ratio of the intensity of the pyrene vibronic bands was decreased with respect to that found in water. This behavior was found for all the studied copolymers, and is in agreement with the location of the fluorescent probe in a hydrophobic microenvironment. In order to determine whether the association of polyelectrolyte chains are predominantly inter- or intramolecular, the effect of the concentration on I_1/I_3 was investigated. Fig. 3 shows results for PN16, where it can be observed that the I_1/I_3 ratio is markedly dependent on the copolymer concentration. The ratio of the intensity of the vibronic bands decreases with increasing the polyelectrolyte concentration. This indicates that the aggregation is related to interchain aggregate formation. Probably, hydrophobic interactions between the aromatic groups of side chains play an important role in the stabilization of interpolymer aggregates.

Fig. 4 shows the AFM topographic images along with the corresponding cross-sections obtained for copolymers adsorbed onto amino-terminated surfaces. Fig. 4a and b correspond to the adsorption of PN16 from 0.001 M NaCl and 0.1 M NaCl solutions, respectively. In both cases the chains seem to be densely packed. The mean roughness values (Table 3) are similar. Fig. 4c and d correspond to PPh16 adsorbed from 0.001 M NaCl and 0.1 M NaCl solutions, respectively. The latter presents a smooth ($rms = 0.4 \pm 0.1$ nm) finely structured layer, while the former is rougher ($rms = 2.2 \pm 0.3$ nm). Similarly, AFM images obtained for PN1250 from 0.001 M NaCl and 0.1 M NaCl solutions, indicate that upon increasing the ionic strength, the surface became smoother. The difference between the rms values found for layers adsorbed at 0.1 mol/L and 0.001 mol/L NaCl is small and corroborates with the contact angle hysteresis, which under low and high ionic strengths amounts to 35° and 32° respectively. AFM images obtained for PPh1250 presented features (images not shown) similar to those above described. Structures as large as those observed by DLS in solution (from 80 nm to 300 nm) could not be observed in any of the adsorbed layers, as revealed by the cross-sections analyses performed for the topographic AFM images.

These findings allow us to propose a model to describe the adsorption behavior of these systems, as depicted in Scheme 3. In solution amphiphilic polyelectrolytes form aggregates that are in equilibrium with free chains. Both free chain and aggregate expose negative charge to the solution, avoiding contact of naphtyl or phenyl groups with water. The adsorption of first layer is driven by electrostatic interaction between negatively charged groups of free polymer chain and positively charged amino-terminated surface.

Table 3
Advancing (θ_a) and receding (θ_r) contact angles, hysteresis ($\Delta\theta$) in the contact angle and mean roughness values (rms) determined by means of AFM images (1 μm × 1 μm) for PPh16, PPh1250, PN16 and PN1250 adsorbed onto amino-terminated surfaces at 0.001 mol/l and 0.1 mol/L NaCl.

C_{NaCl} [mol/L]	Polyelectrolyte[a]	θ_a[°]	θ_r [°]	$\Delta\theta$ [°]	rms [nm]
0.1	PPh16	58 ± 2	37 ± 2	21 ± 2	0.4 ± 0.1
	PPh1250	60 ± 3	36 ± 2	24 ± 3	0.9 ± 0.2
	PN16	61 ± 3	36 ± 3	25 ± 3	0.6 ± 0.1
	PN1250	62 ± 2	30 ± 3	32 ± 3	0.9 ± 0.4
0.001	PPh16	68 ± 2	36 ± 2	32 ± 2	2.2 ± 0.3
	PPh1250	51 ± 3	30 ± 2	21 ± 3	1.0 ± 0.2
	PN16	46 ± 3	26 ± 3	20 ± 3	0.6 ± 0.1
	PN1250	74 ± 2	39 ± 2	35 ± 2	1.5 ± 0.4

[a] $C_p = 0.4$ g/L.

For this layer, high ionic strength helps charge screening and favors the adsorption of chains in a flat conformation, decreasing the Γ values. The first adsorbed layer exposes naphthyl or phenyl hydrophobic groups to the solution. The subsequent adsorbing layer is driven by hydrophobic interaction between phenyl or naphthyl groups on the surface and those from arriving free chains. This second adsorbed layer should expose carboxylate groups to the solution, which repels the arriving chains. Upon drying some hydrophobic groups might be oriented to the air, which is also hydrophobic. This re-orientation agrees with the contact angles between (46 ± 3)° and (74 ± 2)° (Table 3).

3.2. Desorption experiments

In order to investigate the stability of adsorbed polyelectrolyte chains onto amino-terminal surfaces, the copolymers at 0.4 g/L and in 0.1 M and 0.001 M NaCl solutions were allowed to adsorb until adsorption equilibrium. Then, samples were dipped into water or NaCl solution and thickness was monitored. No desorption or change in the thickness layer could be observed after 72 h. This means that interactions between the amino-terminal surface and the polyelectrolyte chains are stable. Moreover, part of the amino-terminal surface positive charges remained even when the pH was increased to ~6.5.

3.3. Influence of the functional group and the chain length on the adsorbed amount

Fig. 2 shows that at low and high ionic strength, $\Gamma_{plateau}$ values for the PN copolymers are independent on the chain length. Meanwhile, the maximum adsorbed amount for PPh copolymers is higher for the compounds with shorter chain length. The plateau for PPh16 is 25% larger than that obtained for PPh1250 copolymer. This finding can be explained on the basis of the side group structure. The naphthyl group is bulkier than phenyl group, and in addition the naphthyl moiety presents a more rigid structure and larger steric hindrance. Therefore, naphthyl modified polyelectrolytes are expected to present a reduced ability to

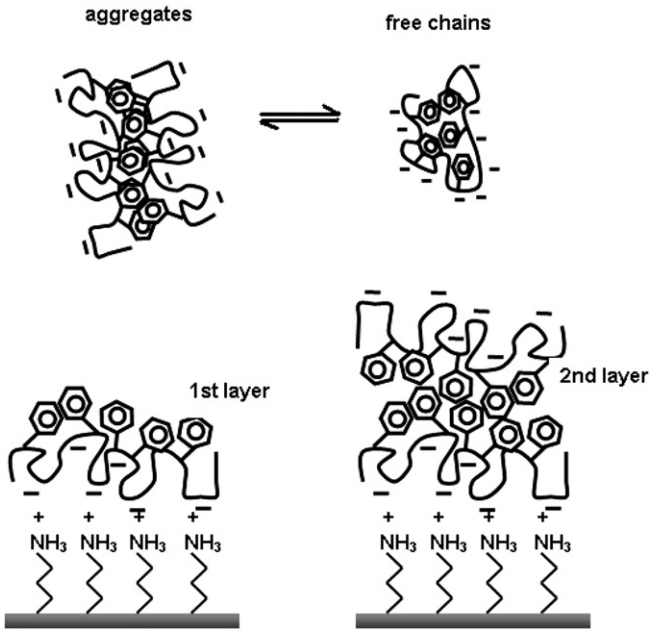

Scheme 3. Proposed model for polyelectrolyte adsorption onto Amino-terminated surface.

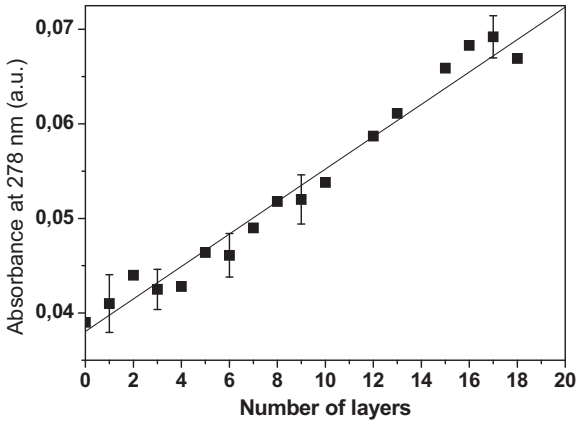

Fig. 5. Absorbance at 278 nm as function of the number of deposited layers. CH and PPh16 were deposited alternately onto amino-terminated quartz slides. The linear fit yielded $y = 0.037 + 0.00175$ x, $R = 0.986$.

accommodate itself on the surface, leading to a lowest adsorption, independently on the chain length. However, when the functional group is phenyl, it is observed the effect of chain length on $\Gamma_{plateau}$ values. Considering that the short PPh16 chains have less flexible conformation, the ability to extend its side chain on the surface is diminished compared to the PPh long chain, probably the conformation where the steric hindrance prevails is compact. In addition, for similar size, at low ionic strength, the $\Gamma_{plateau}$ value is larger when the side chain polyelectrolyte functional group is phenyl. This difference could be attributed to the conformation that the polyelectrolyte adopts on the surface. According to the latter we can conclude that increasing polyelectrolyte hydrophobicity the adsorption is less favorable. On the other hand, at high ionic strength, the effect of the functional group is observed only in the short length chain copolymer. This is in agreement with the screen of the carboxylate groups leading to hindrance surface adsorption. Samoshima et al. [41] found a similar behavior for the adsorption of hydrophobically modified cationic poly(acrylamides) onto silicon surface. These authors suggested that the introduction of hydrophobic groups in cationic poly(acrylamides) has little influence on the adsorbed amount. However, they found that at higher charge density (10% charged groups) the presence the hydrophobic moiety seems to decrease the adsorbed amount.

The dried of the adsorbed polyelectrolytes onto the amino-terminated surface were characterized by contact angle measurements. The advancing (θ_a) and receding (θ_r) contact angles, and the hysteresis ($\Delta\theta$) for the different copolymers are included in Table 3. These values show that independently of the polymer structure θ_a, θ_r and $\Delta\theta$ values did not vary substantially when the layer was formed from 0.1 M NaCl solutions. The similar values of θ_a indicate that upon drying some hydrophobic groups (phenyl and naphthyl) tend to be exposed to the air. The copolymer layers formed from 0.001 M NaCl solutions presented θ_a values ranging from 46 ± 3 for PN16 to 74 ± 2 for PN1250, indicating the tendency of longer polyelectrolytes chains to expose the hydrophobic residues to air. However, the PPh copolymers layers presented minor variations. As proposed in Scheme 3, in solution the second adsorbed layer present carboxylate groups oriented to the medium. Drying favors the exposition of some hydrophobic groups to the air, leading to chemical heterogeneity, which is revealed by the large hysteresis values (Table 3). On the other hand, regardless the ionic strength the hysteresis here found for the adsorption on the amino-termined surfaces is higher than that reported for APS monolayer [22]. This result indicates that the films of polyelectrolytes adsorbed onto the amino-terminated groups are more rugged than that adsorbed onto APS monolayers.

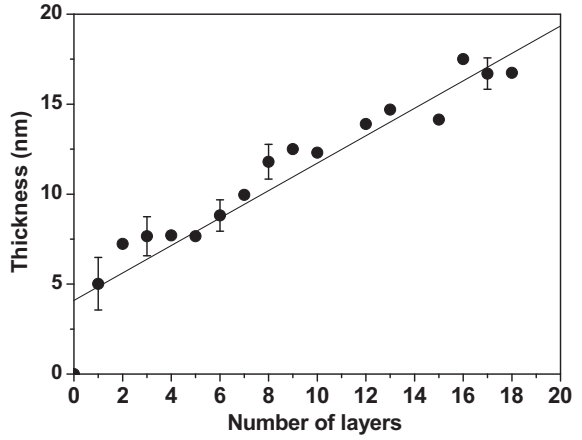

Fig. 6. Thickness as a function of the number of deposited layers. CH and PPh16 were deposited alternately onto amino-terminated Si wafers. The linear fit is $y = 4.19 + 0.763$ x, $R = 0.951$.

3.4. Building-up of multilayers

The results here obtained for copolymer adsorbed on amino-terminated surface show the presence of hydrophobic and hydrophilic areas (Scheme 3). This functional versatility makes these films very attractive for scientific and technological studies, and opens the possibility for layer-by-layer build-up. With this aim we used chitosan (under acidic conditions) as polycation and PPh16 as polyanion. We choose this copolymer because it yields the highest adsorbed amount onto amino-terminated surfaces (see Fig. 2). CH is a linear copolymer of D-glucosamine and *N*-acetyl-D-glucosamine linked in $\beta(1 \rightarrow 4)$, usually derived from the natural polymer chitin. Chitosan has been subject of many studies, due to its good biocompatibility, biodegradability, low toxicity, haemostatic potential [42], good film forming character [43], and anti-infectional activity [44].

The alternated adsorption of CH and PPh16 was conveniently followed by UV spectroscopy. A plot of the absorbance at 278 nm as a function of the number of layers deposited is presented in Fig. 5. The linear dependence of absorbance with the number of adsorbed layers yielded a slope of 0.0018 absorbance units per layer. Film growth was also monitored by ellipsometry, as shown in Fig. 6. A plot of the ellipsometric thickness as a function of the deposition number was fitted by a linear regression, giving a thickness of 0.76 nm for monolayer. Although PPh16 chains carry hydrophobic side groups, the layer-by-layer deposition was successful. Electrostatic interaction between the CH protonated amino groups and PPh16 carboxylate groups contributed to the multilayers build up. Although, hydrogen bonding between CH hydroxyl and PPh16 carbonyl groups should be considered. Similar behavior has been recently reported for the adsorption layer-by-layer films based on amphiphilic polysaccharides [45].

4. Conclusions

The adsorption of functionalized anionic amphiphilic polyelectrolytes, alternated copolymers of maleic anhydride and styrene, onto amino-terminated surfaces is driven by electrostatic interactions. The polyelectrolyte amount adsorbed decreases with ionic strength, in agreement with the *screening-reduced adsorption* regime. In solution amphiphilic polyelectrolytes form aggregates, those are in equilibrium with free chains. A first layer of free polyelectrolyte chains could be adsorbed, onto amino-terminated

surface driven by electrostatic interactions. This thin layer forms a "new substrate" with hydrophobic (naphthyl or phenyl) groups expose to the medium. The assembling of the arriving chains to the already existing monolayer might be driven by interactions between aromatic side groups. The second adsorbed copolymer layer exposes carboxylate groups to the medium, which repels free copolymer chains but attracts chitosan chains.

No effect of the polyelectrolyte chain length on $\Gamma_{plateau}$ value is observed, when copolymers carry naphtyl as side group. The bulkier naphthyl group would confer a more rigid structure, and a larger steric hindrance to the polymer chain, and than reduces its ability to accommodate on the surface. This is in agreement with the fact that at low ionic strength, the $\Gamma_{plateau}$ values are higher for phenyl than naphthyl. Therefore, upon increasing polyelectrolyte hydrophobicity the adsorption onto amino-terminated surface is unfavored.

Acknowledgments

Project Fondecyt N° 1070857 (Chile) and Research Grants C/14036-14, CNPq and FAPESP (Brazilian Foundations) is gratefully acknowledged. We thank María Luz Peña and Guilherme da Silva Gomes for technical support. We thank the Laboratory of Physical Chemistry of Macromolecule and Surface of Dra. L. Gargallo, Dr. D. Radic, and Dr. A. Leiva for the access to Dynamic Light Scattering.

References

[1] Tripathy SK, Kumar J, Nalga HS. Handbook of polyelectrolytes and their application, vol. 2. California: American Scientific Publishers; 2002. 1–63.
[2] Cañete P, Ríos HE, Vargas V, Ronco S, Isaacs M, Urzúa MD. J Colloid Interface Sci 2008;38:183–7.
[3] Tanford C. The hydrophobic affect: formation of micelles and biological membranes. New York: John Wiley & Sons; 1980.
[4] Laschewsky A. Adv Polym Sci 1995;24:3–59.
[5] Chialvo A, Simonson JM. J Mol Liquids 2007;134:15–22.
[6] Olea AF, Barraza RG, Fuentes I, Acevedo B, Martínez F. Macromolecules 2002;35:1049–53.
[7] Yin X, Stöver DH. Macromolecules 2002;35:10178–81.
[8] Auzély-Velty R, Cristea M, Rinaudo M. Biomacromolecules 2002;3:998–1005.
[9] Fang W, Cai Y, Chen X, Su R, Chen T, Xia N, et al. Bioorg Med Chem Lett 2009;19:1903–7.
[10] Urzúa M, Mendizábal FJ, Cabrera WJ, Ríos HE. J Colloid Interface Sci 2005;281:93–100.
[11] Henry SM, El-Sayed M, Pirie CM, Hoffman AS, Stayton PS. Biomacromolecules 2006;7:2407–14.
[12] Decher G, Schlenoff JB. Multilayer thin film. Weinheim: Wiley-VCH; 2003.
[13] Caruso F, Trau D, Möhwald H, Renneberg R. Langmuir 2000;16:1485–8.
[14] Claesson PM, Poptoshev E, Blomberg E, Dedinaite A. Adv Colloid Interface Sci 2005;114-115:173–87.
[15] Dobrynin AV, Rubinstein M. Prog Polym Sci 2005;30:1049–118.
[16] Mishael Y, Dubin P. Environ Sci Technol 2005;39:8475–80.
[17] Arbós P, Arangoa MA, Campanero MA, Irache JM. Int J Pharmaceutics 2002;242:129–36.
[18] Shimomura M, Sawadaishi T. Curr Opin Colloid Interf Sci 2001;6:11–6.
[19] Matsuzawa S, Maneerat C, Hayata Y, Hirakawa T, Negishi N, Sano T. Appl Catal B Environ 2008;83:39–45.
[20] Enarsson L-E, Wägberg L, Carlén J, Ottosson N. Colloids Surf A Physicochem Eng Asp 2009;340:135–42.
[21] Tsapikouni TS, Missirlis YF. Mater Sci Eng B 2008;152:2–7.
[22] Petri DFS, Wenz G, Schunk P, Schimmel T. Langmuir 1999;15:4520–3.
[23] Styrkas DA, Bütün V, Lu JR, Keddie JL, Armes SP. Langmuir 2000;16:5980–6.
[24] Tsukruk VV, Bliznyuk VN, Visser D, Campbell AL, Bunning TJ, Adams WW. Macromolecules 1997;30:6615–25.
[25] Samoshina Y, Nylander T, Lindman B. Langmuir 2005;21:4490–502.
[26] Samoshina Y, Nylander T, Claesson P, Schillen K, Iliopoulos I, Lindman B. Langmuir 2005;21:2855–64.
[27] Li F, Balaste M, Schorr P, Argillier J-F, Yang J, Mays J, et al. Langmuir 2006;22:4084–91.
[28] Pradier CM, Humbolt V, Stievano L, Méthvier C, Lambert JF. Langmuir 2007;23:2463–71.
[29] Fujimoto J, Petri DFS. Langmuir 2001;17:56–60.
[30] Silva RA, Urzúa MD, Petri DFS. J Colloid Interface Sci 2009;330:310–6.
[31] Van de Steeg HGM, Cohen Stuart MA, de Keizer A, Bijsterbosch B. Langmuir 1992;8:2538–46.
[32] Ohno N, Nitta K, Makino S, Sugai N. J Polym Sci Part A Polym Phys 1973;11:413–25.
[33] Roberts GAF, Domszy JG. Int J Biol Macromol 1982;4:374–7.
[34] Azzam RMA, Bashara NM. Ellipsometry and polarized light. Amsterdam: North Holland Publication; 1987.
[35] De Feijter JA, Benjamins J, Veer FA. Biopolymers 1978;17:1759–72.
[36] Motschmann H, Stamm M, Toprakcioglu C. Macromolecules 1991;24:3681–8.
[37] Handbook of chemistry and physics. 64th ed. Boca Raton, Florida: CRC Press; 1984.
[38] Talbot J, Tarjus G, Van Tassel PR, Viot P. Colloids Surf A Physicochem Eng Asp 2000;165:287–324.
[39] Almeida A, Salvadori MC, Petri DFS. Langmuir 2002;18:6914–20.
[40] Pancera SM, Alvarez EB, Politi MJ, Gliemann H, Schimmel T, Petri DFS. Langmuir 2002;18:3517–23.
[41] Samoshima Y, Díaz A, Becker Y, Nylander T, Lindman B. Colloids Surf A Physicochem Eng Asp 2003;231:195–205.
[42] Vasiliu S, Popa M, Rinaudo M. Eur Polym J 2005;41:923–32.
[43] Caseli L, dos Santos D, Foschini M, Goncalves D, Oliveira ON. J Colloid Interface Sci 2006;303:326–31.
[44] Vieira DB, Lincopan N, Mamizuka E, Petri DFS, Carmona-Ribeiro AM. Langmuir 2003;19:924–32.
[45] Guyomard A, Nysten B, Muller G, Glinel K. Langmuir 2006;22:2281–7.